

BIOCONVECTION EFFECTS ON NON-NEWTONIAN CHEMICALLY REACTING WILLIAMSON NANOFUID FLOW DUE TO STRETCHED SHEET WITH HEAT AND MASS TRANSFER[†]

✉ Muhammad Jawad^{*,a}, ✉ M. Muti-Ur-Rehman^b, ✉ Kottakkaran Soopy Nisar^{c,d}

^aDepartment of Mathematics, The University of Faisalabad, Faisalabad 38000, Pakistan

^bDepartment of Mathematics and Statistics University of Agriculture Faisalabad, Faisalabad 38000 Pakistan

^cDepartment of Mathematics, College of Science and Humanities in Alkharj, Prince Sattam Bin Abdulaziz University, Alkharj 11942, Saudi Arabia

^dSchool of Technology, Woxsen University-Hyderabad-502345, Telangana State, India

*Corresponding Author E-mai: muhammad.jawad@uf.edu.pk

Received March 29, 2023; revised April 18, 2023; accepted April 24, 2023

The aim of this paper is to scrutinize the mixed convective flow of Williamson nanofluid in the presence of stretched surface with various physical effects. The impact of Brownian motion and thermophoresis is the part of this investigation. In addition, the features of thermal radiations is considered in energy equation for motivation of problem. Theory of the microorganism is used to stable the model. Mathematical modelling is carried out. Appropriate similarity functions are used to transform the couple of governing PDEs into set of ODEs. Wolfram MATHEMATICA is engaged to solve transformed equations numerically with the help of shooting scheme. The influence of emerging flow parameters like magnetic, thermophoresis, porosity, Péclet and Lewis number on the velocity, temperature, volumetric concentration and density of microorganism distribution are presented in tables and graphs.

Keywords: Gyrotactic Microorganism; Williamson nanofluid; MHD; Bioconvection; Shooting method.

PACS: 44.10.+i, 44.05.+e, 44.30.+v, 47.10.ad.

1. INTRODUCTION

Fluid mechanics have two principal types of fluids called Newtonian and non-Newtonian fluid flow belongings of Newtonian and non-Newtonian fluids are not similar. Newtonian fluids are those which satisfy Newton law of viscosity like water, glycerol, alcohol and benzene. Here, the contact between strain rates is explained by taking out the basic model, especially for such liquids that do not obey the Newton law of viscosity. Fluids like toothpaste, cosmetics, butter, ketchup, custard, shampoo, blood, honey, paint are the examples of non-Newtonian fluids in daily life. Because of the complicated and interdisciplinary nature, the study of non-Newtonian fluids has recently involved a lot of attention from researchers. Nanofluids are small-sized solid particles dissolved in conventional processing fluids. Water, glycerol, engine oils, ethylene glycol, and pump oil are conventional processing fluids. Nanoparticles, which are normally recycled in nanofluids are made from various materials, such as metals or non-metals. Choi and Eastman [1] found that by suspending metallic nanoparticles in traditional fluids, the resulting nanofluids have predicted high thermal conductivity. The movement of heat transfer in a fluid will enhance the conduction and convection coefficients. Nanofluid research is becoming more important and effective. Nanofluids are developed to achieve maximal thermal properties at the smallest concentration possible. The production of nanofluids resulted in increased thermal conductivity and improved heat transfer properties. The transmission qualities and heat conduction characteristics of the base fluids, such as organic, refrigerant, and ethylene liquids, are altered by all non-metallic and metallic particles. In fact, while higher thermal conductivity is dependent on nanoparticles, the efficacy of heat transfer enhancement is also dependent on scattered particles, material type, and other parameters. Using additives to improve a base fluid's heat transfer capacity is another option. Nanofluids have a wide variety of applications and they can be used in different sectors, including heat transferring and other cooling applications. In the biological and biomedical sectors, nanofluids have played vital roles for a long time, and their use will be extended to growth. Nanofluids have also been used as detergents and smart fluids. Jawad et al. [2] has inspected that nanofluid is such kinds of hotness move source having nano-particles with shape short 100 (nm). Wen and Ding [3] have found that nanofluids significantly improved convective heat transfer, according to the findings. The improvement was especially noticeable in the entrance region, and it was much greater than the increase in thermal conduction. The classical Such equation was also shown to be ineffective in predicting the heat transfer conduct of nanofluids. The main explanations were proposed to be nanoparticle migration and the commotion of the boundary layer. Bhattacharya *et al.* [4] have evaluated the thermal conductivities of aluminium oxide-water nanofluids at different temperatures and clarify that the enhancement in thermal conductivity is temperature dependent.

Magnetohydrodynamics, also known as hydro-magnetics, is the learning of dynamics of the existence of magnetic properties and the liquid effects that are electrically conducted. Salt water, liquid metals, plasma and electrolytes are known examples of magneto fluids. Alfvén [5], a Swedish physicist, was the first to introduce the MHD fluid flow. Turkyilmazoglu [6] has calculated analytically the magnetohydrodynamic flow and thermal transport features of nanofluid flow across a continually extending or contracting permeable sheet in the presence of temperature and velocity

[†] Cite as: M. Jawad, M.M. Ur-Rehman, and K.S. Nisar, East Eur. J. Phys. 2, 359 (2023), <https://doi.org/10.26565/2312-4334-2023-2-42>

© M. Jawad, M. M.-Ur-Rehman, K.S. Nisar, 2023

slip. Qayyum *et al.* [7] have observed analytical treatment of MHD radiative flow of tangential hyperbolic nanofluid under the impact of heat generation or absorption. The study's reproduction was based on Newtonian heat and mass conditions. Mohyud-Din *et al.* [8] have presented a revised model for Stokes first issue in nanofluids. At the boundary, this model considers a zero-flux condition. Following the implementation of the similarity transforms, the governing equations were altered into a system of non-linear ordinary differential equations. Majeed *et al.* [9] has concentrated on that Magneto hydrodynamics manages electrically led liquid having attractive properties in like manner of electrolytes, salt water, plasmas, and fluid metals. Nadeem *et al.* [10] have studied the Casson fluid's MHD boundary layer movement across an increasingly permeable shrink sheet.

Williamson [11] concentrated on the progression of pseudoplastic materials and fostered a model to clarify the progression of liquids and gave trial results. In the Williamson model, the compelling consistency ought to be decreased endlessly by raising the shear rate, which is boundless thickness very still and no consistency as the shear rate approaches endlessness. The Williamson liquid model is an essential reenactment of non-Newtonian liquid viscoelastic shear diminishing highlights. Hayat *et al.* [12] have analysed the results of chemically reactive flow of nanomaterial based on Brownian and Thermophoresis movement with a nonlinear bidirectional stretching layer with a constant thickness. Williamson fluid rheological expressions and the optimal homotopy analysis approach were used. Zaman and Gul [13] have examined in the presence of Newtonian conditions, the magneto hydrodynamic (MHD) of Williamson nanofluid bioconvective flow containing microorganisms. The bvp4c technique is used to achieve numerical solutions. Danish *et al.* [14] have explained a new numerical model to analyse the features of activation energy on magnetized Williamson fluid over a section with nonlinear thermal radiation. The Brownian and thermophoresis nanofluid properties have been described using the Buongiorno model. For more details see Refs [15-23].

Kuznetsov [24] were the first to investigate the topic of bioconvection in a suspension containing small solid particles (nanoparticles). To see how minor particles that are denser than water affect the permanence of a motile gyrotactic bacteria suspension in a finite-depth horizontal fluid layer. Bioconvection has the potential to improve mass transport and mixing, particularly in microvolumes, as well as the stability of nanofluids. Thus, a nanofluid and bioconvection combination could be promising for new microfluidic devices. Khan *et al.* [25] have explained the movement over a permeable wedge in the occurrence of viscous dissipation and Joule heating. The nanofluid containing gyrotactic microorganisms was expected to be saturated in the wedge under the effect of magneto-hydrodynamics. The passive control model was used to formulate the problem. Uddin *et al.* [26] have evaluated numerically the impacts of bioconvection on fluid velocity and thermal slips over the flow of nanofluid passing through the horizontal touching sheet. They introduced the first time-similarity solution to nano-bioconvection. The influences of velocity, the bioconvection Lewis number, Peclet number and the bioconvection Peclet number on the governing equations, including local wall mass flux and local Nusselt number, were discussed. Naz *et al.* [27] have reviewed Cross nanofluid with gyrotactic germs, entropy formation and heat and mass transmission. The solutions were obtained using the optimal homotopy analysis technique, and the most important consequences were discussed graphically and numerically. The geometry of flow model is presented in Fig. 1 as:

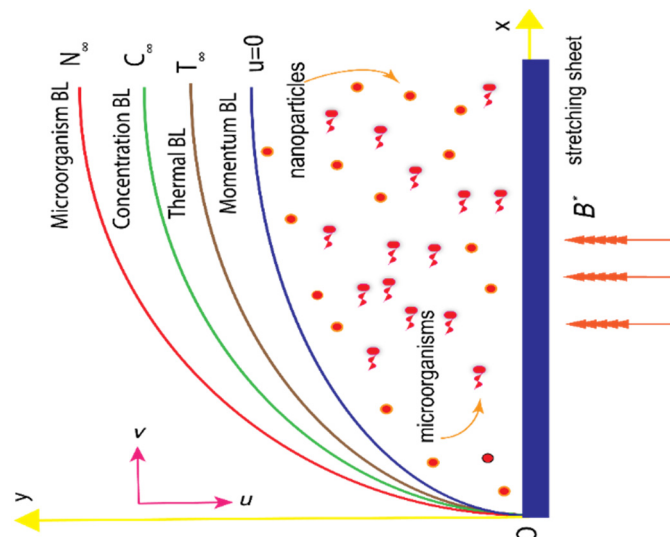


Figure 1. Geometry of physical model

2. PROBLEM STATEMENT

A mathematical study of MHD flow of an incompressible Williamson nanofluid is presented. The two-dimensional fluid flow is passing through porous media and stretched surface. Aman *et al.* [28] work of mixed convection nanofluid flow with gyrotactic microorganisms over extending plate has been considered. The first step is to explore this work and then extending that by observing the consequence of magnetic field, thermal radiation and chemical reaction with compactness of motile microorganisms.

The governing equations [29] are:

$$u_x + v_y = 0 \tag{1}$$

$$uu_x + vu_y = \nu u_{yy} - \frac{\sigma_e B_0^2 u}{\rho_f} + \Gamma u_y u_{yy} \tag{2}$$

$$uT_x + vT_y = \frac{k}{(\rho c)_f} (T_{yy}) + \frac{(\rho c)_p}{(\rho c)_f} \left\{ \frac{D_T}{T_\infty} (T_y)^2 + D_B C_y T_y \right\} \tag{3}$$

$$uC_x + vC_y = D_B C_{yy} + \frac{D_T}{T_\infty} T_{yy} - K_0 (C - C_\infty) \tag{4}$$

$$un_x + vn_y + \frac{bW_c}{C_w - C_\infty} [n_y C_{yy}] = D_m n_{yy} \tag{5}$$

Conditions:

The initial and boundary conditions [30] are

$$v = v_0, u = \lambda U_w, T = T_w, C = C_w, N = N_w \text{ at } y = 0, \tag{6}$$

$$u \rightarrow 0, T \rightarrow T_\infty, C \rightarrow C_\infty, N \rightarrow N_\infty \text{ as } y \rightarrow \infty,$$

Similarity transformations:

$$u = bx f'(\eta); v = -(bv)^{\frac{1}{2}} f(\eta); \eta = \sqrt{\frac{b}{\nu}} y; \phi(\eta) = \frac{C - C_\infty}{C_w - C_\infty}; \chi(\eta) = \frac{N - N_\infty}{N_w - N_\infty} \quad \theta(\eta) = \frac{T - T_\infty}{T_w - T_\infty}.$$

3. NUMERICAL SCHEME: SHOOTING METHOD

The physical aspect of the flow problem under consideration has been investigated by solving the final set of equations, namely (2) to (5) associated with the new boundary conditions (6). The policy of shooting method is specified as next (Fig. 2). The higher order derivatives in the above mentioned are reduced to first order as follows:

$$f'''(\eta) + \lambda f''(\eta) f'(\eta) + f''(\eta) f(\eta) - f'^2(\eta) - M f'(\eta) = 0, \tag{7}$$

$$\theta''(\eta) + Pr f(\eta) \theta'(\eta) - 2Pr \theta(\eta) + \frac{Nc}{Le} \phi'(\eta) \theta'(\eta) + \frac{Nc}{(Le)(Nbt)} \theta'^2(\eta) = 0, \tag{8}$$

$$\phi''(\eta) + \frac{1}{Nbt} \theta''(\eta) + Sc f(\eta) \phi'(\eta) - Sc \gamma \phi(\eta) = 0, \tag{9}$$

$$\chi''(\eta) + Sc f(\eta) \chi'(\eta) - Pe [\chi'(\eta) \phi'(\eta) + (\chi(\eta) + \sigma) \phi''(\eta)] = 0. \tag{10}$$

The higher order equation from (7) to (10) are reduced to first order as

$$f' = u, u' = v, \theta' = w, \phi' = q, \chi' = g, \tag{11}$$

$$v'(1 + \lambda v) + v f - u^2 - M u = 0, \tag{11}$$

$$w' + Pr f w - 2Pr \theta + \frac{Nc}{Le} q w + \frac{Nc}{(Le)(Nbt)} w^2 = 0, \tag{12}$$

$$q' + \frac{1}{Nbt} w' + Sc f q - Sc \gamma \phi = 0, \tag{13}$$

$$g' + Sc f g - Pe [g q + (\chi + \sigma) q'(\eta)] = 0. \tag{14}$$

The transformed linearly boundary condition follows that

$$f(0) = S, f'(0) = \lambda, \chi(0) = 1, \theta(0) = 1$$

$$f'(0) = 0, \theta = 0, \phi = 0, \chi = 0 \text{ as } \eta \rightarrow \infty \tag{15}$$

$$\left\{ \begin{aligned} N_b &= \frac{\tau D_B (C_w - C_\infty)}{\nu}, Nt = \frac{\tau D_T (T_w - T_\infty)}{\nu T_\infty}, Sc = \frac{\nu}{D_n}, \\ Pe &= \frac{bW_c}{D_n}, \sigma = \frac{N_\infty}{N_w - N_\infty}, Pr = \frac{\nu}{\alpha}, \alpha = \frac{k}{(\rho c)_f}, \gamma = \frac{K_0}{a}, Le = \frac{\nu}{D_B}. \end{aligned} \right.$$

The dimensionless drag force factor $Cf_x = \frac{2\tau_w}{\rho_f u_w^2}$, the Nusselt amount $Nu_x = \frac{xq_w}{\alpha_f (T_m - T_\infty)}$, local Sherwood amount

$Sh_x = \frac{xq_s}{D_B(C_w - C_\infty)}$ and density of microorganism's amount $Nn_x = \frac{xq_n}{D_n(N_w - N_\infty)}$ on the surface in x -direction are given by

$$(Re_x)^{1/2} Cf_x = \left[f''(0) + \frac{We}{2} f''(0) \right], (Re_x)^{-1/2} Nu_x = -\theta'(0), (Re)^{-1/2} Sh_x = -\phi'(0), (Re)^{-1/2} Nn_x = -\chi'(0) \quad (16)$$

here is Re_x the Reynold amount.

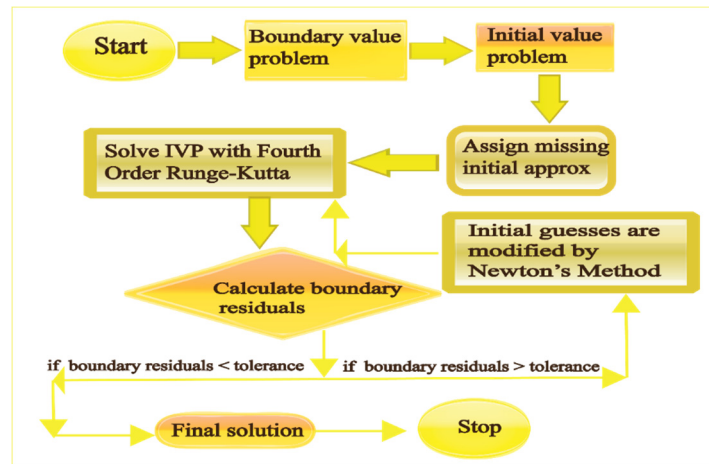


Figure 2. Chart of shooting method steps.

4. CODE VALIDATIONS

Table 1 provides a critical study of the current findings of $-\theta'(0)$ and $-\Phi'(0)$ for the Brownian motion parameter Nbt utilising the `bvp4c`. The critical study of these numerical findings in Table 1 reveals that the scheme is valid, $M = 0.5$, $\lambda = 0.1$, $Pr = 7$, $Nc = \sigma = 0.3$, $Pe = Le = Sc = 0.2$ and $\gamma = 0$. The comparison of findings in Table 1 shows the astonishingly considerable arrangements of the current inquiry with the `bvp4c` results, which motivates the author to tackle this problem with changes of thermal radiation and chemical reaction effects using a well-known shooting approach.

Table 1. Comparing of $-\theta'(0)$ and $-\Phi'(0)$ values with Nbt .

Parameter	bvp4c	Present	bvp4c	Present
Nbt		$-\theta'(0)$		$-\Phi'(0)$
0.1	1.15530	1.15530	0.71014	0.71014
0.2	0.82269	0.82269	0.42568	0.42568
0.3	0.56501	0.56501	0.22571	0.22571
0.4	0.37418	0.37418	0.09420	0.09420
0.5	0.23916	0.23916	0.01731	0.01731

5. RESULT AND DISCUSSION

In the current investigation we analyzed the impact of different parameters graphically on non-layered speed, non-layered liquid temperature, dimensionless liquid focus and non-layered motile microorganism profiles. The principal request arrangement of conditions along with limit and starting conditions is tackled by utilizing the order ND settled on Mathematica. For this, fixed upsides of certain boundaries are picked self-assertively as given in the accompanying: $M = 1$; $S = 2$; $\lambda = 1$; $Sc = 1$; $\sigma = 0.1$; $Nb = 0.5$; $\gamma = 0.1$; $Nt = 0.5$; $Pe = 1$; $Pr = 1$; $Le = 1$; $Nr = 0.5$; $Nc = 0.5$. Further, in this segment we discussed the graphical consequences of the work of (Aman *et al.* [28]). The first order system of equation (7) to (10) together boundary and initial conditions (15) has been resolved by applying the appreciation ND solve on MATHEMATICA version 11. The computational results for velocity, concentration, temperature, and density function of motile micro-organism have been obtained for several interested parametrical values namely magnetic parameter, the injection/suction parameter, Stretching/Shrinking parameters.

The results have been presented in tabular form in Table 2. The impact of suction/injection at the wall on component of velocity, concentration profile, temperature profile and profile of motile micro-organism.

5.1. Velocity Distribution

In this section, we will confer certain flow parameters that are considered in the velocity contour in the form of schemes. The Hartmann number M , section or injection parameter S are plotted against the velocity function f' . The consequence of the parameter S on the velocity profile f' is shown in Fig. 3. As the parametric value of S increases, the curves show decreasing behavior. The impact of shrinking sheet parameter λ' is described in Figs. 4 and 5.

Table 2. Nusselt number, Sherwood number and local density number at the stretching walls.

M	λ	σ	Pe	S	Pr	Nb	Nc	γ	Le	Sc	$Nu_x Re_x^{-1/2}$	$S_x Re_x^{-1/2}$	$Nn_x Re_x^{-1/2}$
1.0	0.3	0.2	2.0	1	1.0	0.3	0.3	0.1	0.4	0.4	1.16658	0.56551	4.32922
2.0											1.15122	0.40949	3.21536
3.0											1.07339	0.16074	1.04171
	0.2										0.17513	0.45781	2.94380
	0.6										0.17227	0.44646	2.85186
	0.8										0.16901	0.41386	2.74917
		0.5									1.13332	0.40569	1.36868
		0.9									1.13332	0.40569	1.41038
		1.3									1.13332	0.40569	1.45209
			1.0								1.13733	0.22029	0.43076
			1.5								1.13733	0.22029	0.47949
			2.0								1.13733	0.22029	0.52877
				1							2.16132	1.43886	4.26399
				2							2.16043	1.43679	4.24718
				3							2.15950	1.43468	4.22998
					1.0						0.45076	0.00965	-0.74796
					2.0						0.68382	-0.08265	-1.23761
					3.0						0.84726	-0.07902	-1.04745
						1					1.15747	0.43020	3.19427
						2					0.82403	0.90843	7.04755
						3					0.56578	1.04347	8.14002
							0.5				1.15741	0.43020	3.19439
							1				0.95048	0.10050	0.67047
							1.5				0.86337	0.02480	0.16696
								0.1			1.15751	0.43030	3.19429
								0.5			1.05197	0.48545	3.63175
								1.0			0.99723	0.51465	3.86423
									0.5		1.08466	0.35128	2.43539
									1.0		0.93458	0.66761	5.01486
									1.5		0.83408	0.97853	7.05758
										1	0.82404	0.90851	7.04754
										2	0.89140	0.75772	5.85982
										3	0.92655	0.68163	5.26338

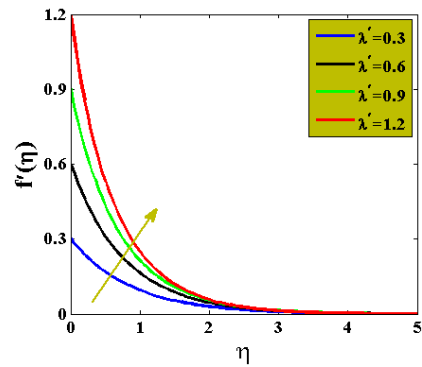
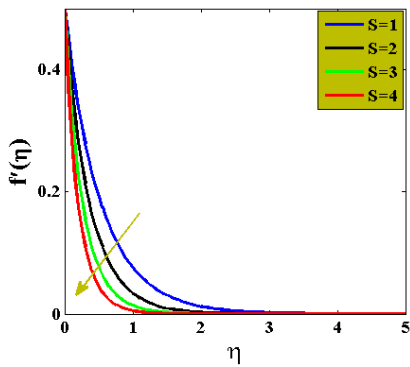


Figure 3. Distribution of velocity profile for some values of S **Figure 4.** Distribution of velocity profile for some values of λ' .

The speed of flow is enhanced and reduced for increasing values of λ' and λ respectively. The sense of parameter M on velocity profile of the fluid is demonstrated by Fig. 6.

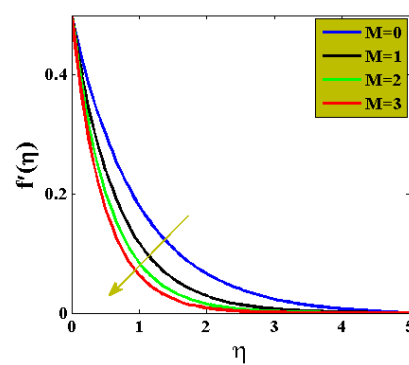
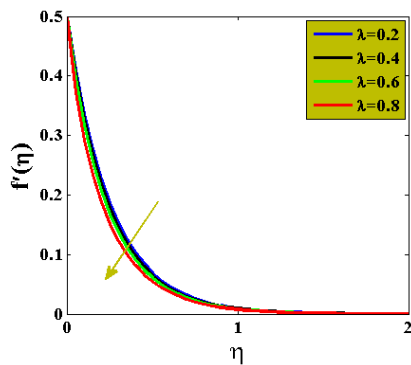


Figure 5. Graph pattern of velocity profile for some values of λ . **Figure 6.** Diagram of velocity profile for some values of M .

These curves show reduction in velocity profile with the cumulative values of M . It is because of the cooperation of restricting powers, to be specific Lorentz power, which is expanded. The Lorentz power is a blend of electric and attractive powers on a moving point charge because of electromagnetic fields. Lorentz powers are resistive powers and are associated with attractive numbers. With the augmentation in, Lorentz power supports up, which goes against the fluid stream because of decrease in the speeds.

5.2. Temperature Distribution

In this section, parametrical effects of diffusivity ratio Nbt , Prandtl number Pr , chemical reaction parameter γ , magnetic parameter M , Lewis number Le , suction or injection parameter S , shrinking sheet parameter λ' , and parameter of heat capacity Nc are depicted in Figs. 7-13. Behavior of temperature profile with deference to parameter S is represented by Fig. 7. When there is gradual increase in the standards of suction or injection parameter S , curves of temperature profile depict deceleration behavior gradually. Fig. 8 illustrates the behavior regarding magnetic parameter on temperature profile.

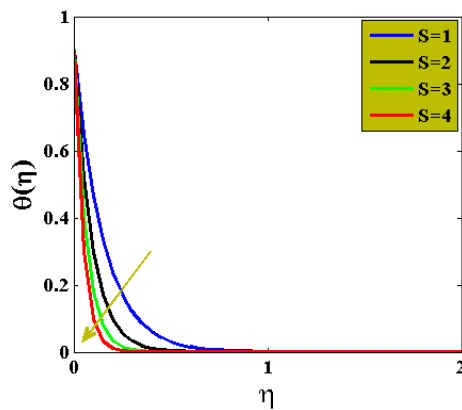


Figure 7. Diagram of temperature profile for some values of S

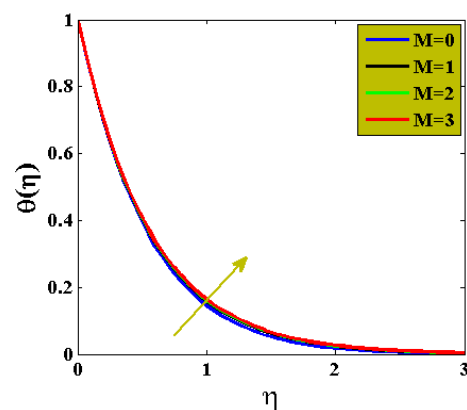


Figure 8. Diagram of temperature profile for some values of M

The graph curves show significant increment in temperature profile with the increasing values of M . Fig. 9 shows the consequence of shrinking parameter λ' on temperature profile. The decrease in the principles of λ' in the stretching case resulted in reducing the temperature contour θ . Fig. 10 is sketched to analyze the influence of Prandtl number Pr on temperature profile, while keeping other parameters constant. Deceleration in temperature field was obtained when increment was done in values of Pr .

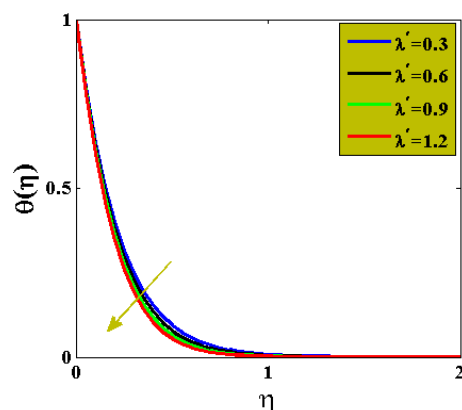


Figure 9. Diagram of temperature profile for some values of λ' .

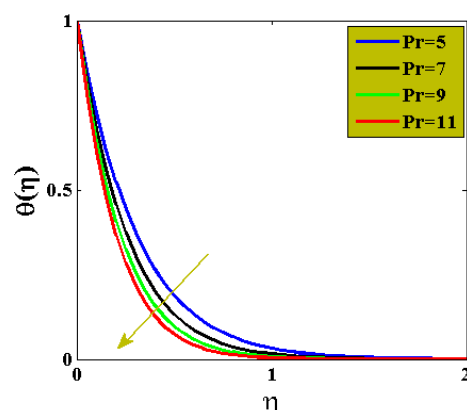


Figure 10. Diagram of temperature profile for some values of Pr .

Fig. 11 is demonstrated to examine the effect of Nc on the temperature profile. When the increment is done in the parametric value of heat capacity ratio, the curves of temperature profile gave an increasing behavior. So, temperature was increased with increasing the heat capacity ratio. Fig. 12 indicates the conduct of temperature profile with respect to parametric values of diffusivity ratio Nbt . When a gradual increment is done in the morals of diffusivity ratio Nbt , deceleration is obtained in the temperature field. Fig. 13 is drawn to summarize the consequence of Lewis number Le on the temperature profile. The curve pattern shows that the increasing Lewis number markedly decreased the temperature profile.

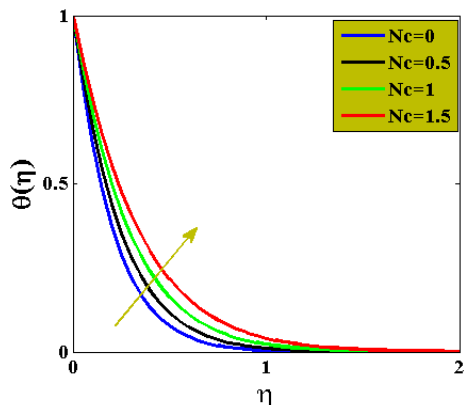


Figure 11. Diagram of temperature profile for some values of N_c

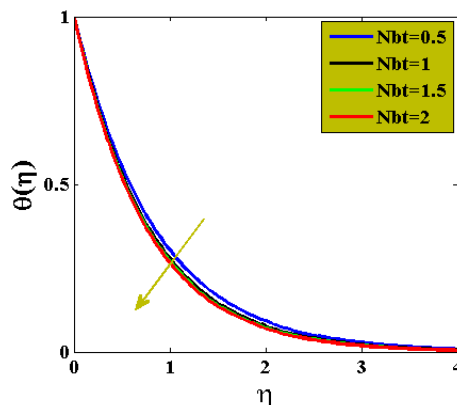


Figure 12. Diagram of temperature profile for some values N_{bt} .

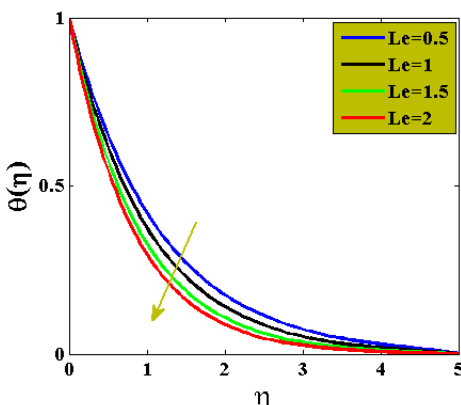


Figure 13. Diagram of temperature profile for some values of Le .

5.3. Concentration Distribution

In this section, influences regarding diffusivity ratio parameter N_{bt} , chemical reaction parameter γ , magnetic parameter M , suction or injection parameter S , shrinking sheet parameter λ' and Schmidt number Sc are depicted on the concentration profile in Figs. 14-19. Fig. 14 displays the effect of stretching or shrinking sheet parameter on concentration profile. On increasing values of λ' , a decreasing behavior of concentration is obtained. In Fig. 15, diffusivity ratio parameter N_{bt} is depicted to show its behaviour on concentration profile.

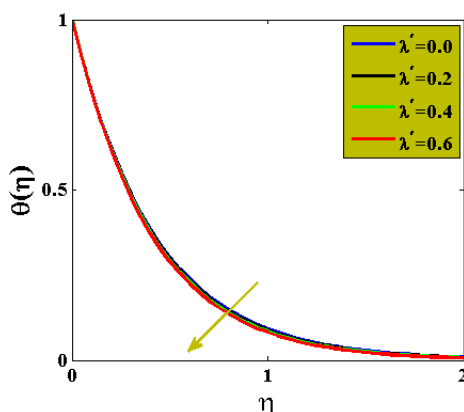


Figure 14. Diagram of concentration profile for some values of λ'

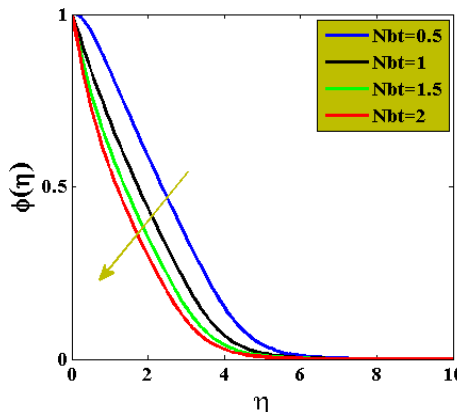


Figure 15. Diagram of concentration profile for some values of N_{bt}

A significant downfall in the curve of concentration profile is obtained when gradual increase is done in diffusivity ratio parameter N_{bt} . Behavior of concentration profile regarding Schmidt number Sc is depicted in Fig.16. When parametrical values of Sc are boosted up, a significant decrease is resulted in concentration profile. Schmidt number is ratio between viscosity and molecular diffusion. Impact of chemical reaction parameter γ on concentration profile is depicted in Fig.17.

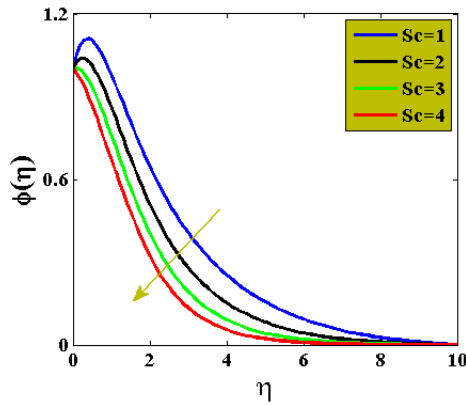


Figure 16. Diagram of concentration profile for some values of Sc .

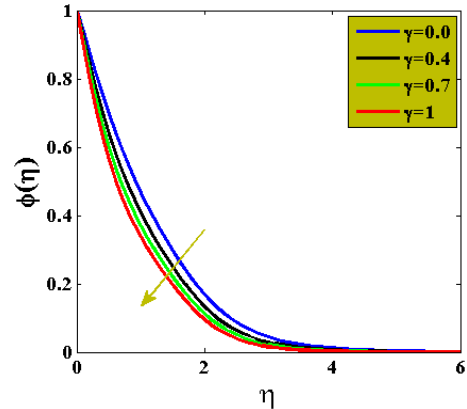


Figure 17. Diagram of concentration profile for some values of γ .

Curve of concentration profile of fluid is decreased when chemical reaction parameter γ is increased. The concentration profile curve with respect to magnetic parameter M is demonstrated in Fig. 18. A remarkable increment is resulted in concentration field when magnetic field parameter is increased. The change in concentration profile for some values of suction or injection parameter S is elaborated in Fig. 19. A decreasing behavior of concentration profile of fluid is obtained with increasing values of S .

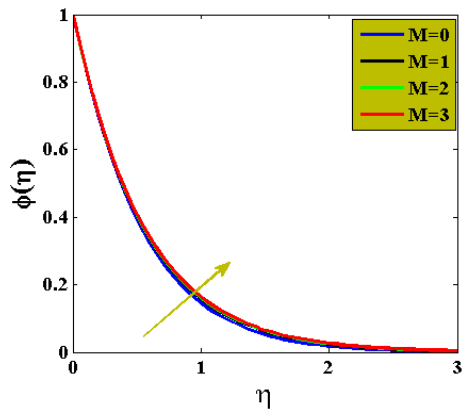


Figure 18. Diagram of concentration profile for some values of M .

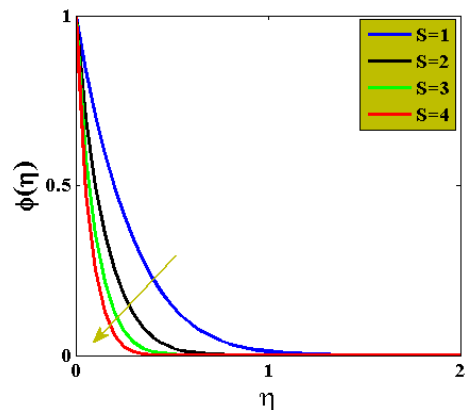


Figure 19. Diagram of concentration profile for some values of S .

5.4. Motile microorganism density Distribution

In this section, effects regarding Schmidt number Sc , Peclet number Pe , σ , and suction or injection parameter S on the density profile of motile micro-organism are discussed in Figs. 20-23. Fig. 20 shows the effect of Peclet number Pe on the density of motile microorganisms. It is observed that increment in the values of Peclet number is caused in increasing the density of motile microorganisms. Fig. 21 shows the effect of parametrical values of suction/injection on the density of motile microorganisms.

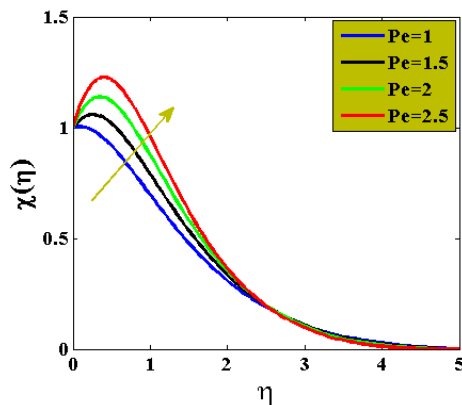


Figure 20. Diagram of motile microorganism profile for some values of Pe .

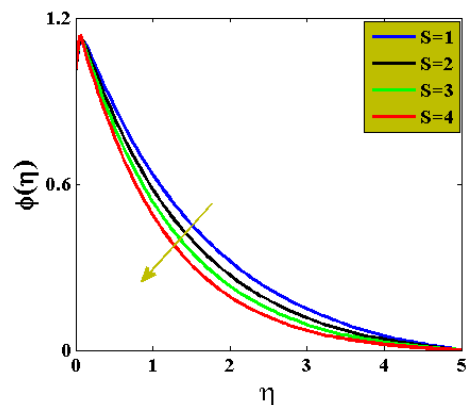


Figure 21. Diagram of motile microorganism profile for some values of S .

According to the plot, deceleration in density is attained for increasing values of S . The graph of Schmidt number Sc on motile density profile is displayed in Fig. 22. Density profile of motile microorganisms is decreased for gradual increase in Schmidt number. Effect of dimensionless parameter σ on density of microorganism is presented in Fig. 23. An important growth is observed in density, when dimensionless parameter σ is increased.

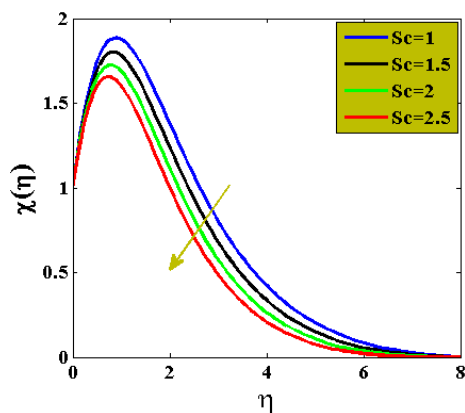


Figure 22. Diagram of motile microorganism profile for some values of Sc .

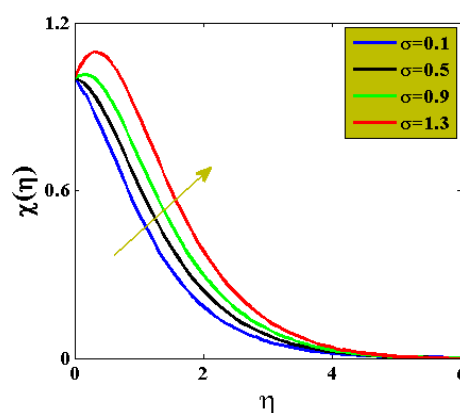


Figure 23. Diagram of motile microorganism profile for some values of σ .

6. CONCLUSION

The main objective is to understand the “radiative effects on MHD Williamson nanofluid flow over a porous stretching sheet with gyrotactic microorganism: Buongiorno's model”. Furthermore, the impacts of chemical reaction, magnetic effect and density of motile microorganism are under assumption. Firstly, useful dimensionless variables are implemented to alter the system of partial differential equations into system of ordinary differential equations. Later on, the approximate solution of transformed boundary value problem is calculated by using shooting scheme for numerically solution by employing ND solving command on Mathematica software. The effects of different physical parameters on non-dimensional velocity function, temperature profile, mass concentration profile and motile microorganism's density function are observed. The principal revelations of this work are as per the following:

- The effect of attractive field is to diminish every one of the actual amounts of interest, where it affected fundamentally on speed work.
- The speed of nanofluids diminishes by expanding attractions boundary S .
- The temperature nanofluids profile increments by expanding Nc .
- The temperature work for nanofluids diminishes by expanding Prandtl number Pr .
- The concentration function decreases by increasing Nb .
- The concentration function decreases by increasing Sc .
- The microorganism density is increased by collective bio convection Peclet number Pe

The shooting method could be applied to a variety of physical and technical challenges in the future [31-35].

Data Availability

All data generated or analyzed during this study are included in this published article.

Conflict of Interest

The authors announce that no conflict of curiosity exists.

Acknowledgement: "This study is supported via funding from Prince Sattam bin Abdulaziz University project number (PSAU/2023/R/1444)"

ORCID IDs

© Muhammad Jawad, <https://orcid.org/0000-0002-9304-615X>; © M. Muti-Ur-Rehman, <https://orcid.org/0009-0008-5572-5208>
© Kottakkaran Sooppy Nisar, <https://orcid.org/0000-0001-5769-4320>

REFERENCE

- [1] S.U. Choi, and J.A. Eastman, Enhancing thermal conductivity of fluids with nanoparticles, Argonne National Lab., IL (United States), **29**, 99-105 (1995). <https://www.osti.gov/biblio/196525>
- [2] M. Jawad, K. Shehzad, R. Safdar, and S. Hussain, “Novel computational study on MHD flow of nanofluid flow with gyrotactic microorganism due to porous stretching sheet,” Punjab University Journal of Mathematics, **52**(12), 43-60 (2020). http://pu.edu.pk/images/journal/math/PDF/Paper_5_52_12_2020.pdf
- [3] D. Wen, and Y. Ding, “Experimental investigation into convective heat transfer of nanofluids at the entrance region under laminar flow conditions,” International journal of heat and mass transfer, **47**, 5181-5188 (2004). <https://doi.org/10.1016/j.jheatmasstransfer.2004.07.012>
- [4] P. Bhattacharya, S. Nara, P. Vijayan, T. Tang, W. Lai, P.E. Phelan, R.S. Prasher, D.W. Song, and J. Wang. “Evaluation of the Temperature Oscillation Technique to Calculate Thermal Conductivity of Water and Systematic Measurement of the Thermal

- Conductivity of Aluminum Oxide–Water Nanofluid,” American Society of Mechanical Engineers Digital Collection, *Heat Transfer*, **2**, 51-56 (2004). <https://doi.org/10.1115/IMECE2004-60257>
- [5] H. Alfven, “Existence of electromagnetic-hydrodynamic waves,” *Nature*, **150**, 405-406 (1942). <https://doi.org/10.1038/150405d0>
- [6] M. Turkyilmazoglu, “Exact analytical solutions for heat and mass transfer of MHD slip flow in nanofluids,” *Chemical Engineering Science*, **84**, 182-187 (2012). <https://doi.org/10.1016/j.ces.2012.08.029>
- [7] S. Qayyum, T. Hayat, S.A. Shehzad, and A. Alsaedi, “Mixed convection and heat generation/absorption aspects in MHD flow of tangent-hyperbolic nanoliquid with Newtonian heat/mass transfer,” *Radiation Physics and Chemistry*, **144**, 396-404 (2018). <http://dx.doi.org/10.1016/j.radphyschem.2017.10.002>
- [8] S.T. Mohyud-Din, U. Khan, N. Ahmed, and M.M. Rashidi, “A study of heat and mass transfer on magnetohydrodynamic (MHD) flow of nanoparticles,” *Propulsion and Power Research*, **7**, 72-77 (2018). <https://doi.org/10.1016/j.jprr.2018.02.001>
- [9] A. Majeed, A. Zeeshan, and M. Jawad, “Double stratification impact on radiative MHD flow of nanofluid toward a stretchable cylinder under thermophoresis and Brownian motion with multiple slip,” *International Journal of Modern Physics B*, **2350232**, (2023). <https://doi.org/10.1142/S0217979223502326>
- [10] S. Nadeem, R. Ul Haq, and C. Lee, “MHD flow of a Casson fluid over an exponentially shrinking sheet,” *Scientia Iranica*, **19**, 1550-1553 (2012). <http://dx.doi.org/10.1016/j.scient.2012.10.021>
- [11] R.V. Williamson, “The flow of pseudoplastic materials,” *Industrial & Engineering Chemistry*, **21**, 1108-1111 (1929). <https://doi.org/10.1021/ie50239a035>
- [12] T. Hayat, M.Z. Kiyani, A. Alsaedi, M. Ijaz Khan, and I. Ahmad, “Mixed convective three-dimensional flow of Williamson nanofluid subject to chemical reaction,” *International Journal of Heat and Mass Transfer*, **127**, 422-429 (2018). <https://doi.org/10.1016/j.ijheatmasstransfer.2018.06.124>
- [13] S. Zaman, and M. Gul, “Magnetohydrodynamic bioconvective flow of Williamson nanofluid containing gyrotactic microorganisms subjected to thermal radiation and Newtonian conditions,” *Journal of Theoretical Biology*, **479**, 22-28 (2019). <https://doi.org/10.1016/j.jtbi.2019.02.015>
- [14] G.A. Danish, M. Imran, M. Tahir, H. Waqas, M.I. Asjad, A. Akgül, and D. Baleanu, “Effects of Non-Linear Thermal Radiation and Chemical Reaction on Time Dependent Flow of Williamson Nanofluid with Combine Electrical MHD and Activation Energy,” *Journal of Applied and Computational Mechanics*, **7**(2), 546-558 (2021). <https://doi.org/10.22055/jacm.2020.35122.2568>
- [15] V. Kumar, S.K. Singh, V. Kumar, W. Jamshed, and K.S. Nisar, “Thermal and thermo-hydraulic behaviour of alumina-graphene hybrid nanofluid in minichannel heat sink: An experimental study,” *International Journal of Energy Research*, **45**(15), 20700-20714 (2021). <https://doi.org/10.1002/er.7134>
- [16] J. Zhang, S.M. Sajadi, Y. Chen, I. Tlili, and M.A. Fagiry, “Effects of Al₂O₃ and TiO₂ nanoparticles in order to reduce the energy demand in the conventional buildings by integrating the solar collectors and phase change materials,” *Sustainable Energy Technologies and Assessments*, **52**, 102114 (2022). <https://doi.org/10.1016/j.seta.2022.102114>
- [17] I. Tlili, and T. Alharbi, “Investigation into the effect of changing the size of the air quality and stream to the trombe wall for two different arrangements of rectangular blocks of phase change material in this wall,” *Journal of Building Engineering*, **52**, 104328 (2022). <https://doi.org/10.1016/j.jobbe.2022.104328>
- [18] X. Qi, M.O. Sidi, I. Tlili, T.K. Ibrahim, M.A. Elkotb, M.A. El-Shorbagy, and Z. Li, “Optimization and sensitivity analysis of extended surfaces during melting and freezing of phase changing materials in cylindrical Lithium-ion battery cooling,” *Journal of Energy Storage*, **51**, 104545 (2022). <https://doi.org/10.1016/j.est.2022.104545>
- [19] J. Alzahrani, H. Vaidya, K.V. Prasad, C. Rajashekhar, D.L. Mahendra, and I. Tlili, “Micro-polar fluid flow over a unique form of vertical stretching sheet: Special emphasis to temperature-dependent properties,” *Case Studies in Thermal Engineering*, **34**, 102037 (2022). <https://doi.org/10.1016/j.csite.2022.102037>
- [20] J. Gao, J. Liu, H. Yue, Y. Zhao, I. Tlili, and A. Karimipour, “Effects of various temperature and pressure initial conditions to predict the thermal conductivity and phase alteration duration of water-based carbon hybrid nanofluids via MD approach,” *Journal of Molecular Liquids*, **351**, 118654 (2022). <https://doi.org/10.1016/j.molliq.2022.118654>
- [21] R.T. Mahmood, M.J. Asad, S.H. Hadri, M.A. El-Shorbagy, A.A.A. Mousa, R.N. Dara, M. Awais, and I. Tlili, “Bioremediation of textile industrial effluents by Fomitopsis pinicola IEBL-4 for environmental sustainability,” *Human and Ecological Risk Assessment: An International Journal*, **29**(2), 285-302, (2023). <https://doi.org/10.1080/10807039.2022.2057277>
- [22] M.K. Nayak, F. Mabood, A.S. Dogonchi, K.M. Ramadan, I. Tlili, and W.A. Khan, “Entropy optimized assisting and opposing non-linear radiative flow of hybrid nanofluid,” *Waves in Random and Complex Media*, 1-22 (2022). <https://doi.org/10.1080/17455030.2022.2032474>
- [23] K.M. Ramadan, O. Qisieh, and I. Tlili, “Thermal creep effects on fluid flow and heat transfer in a microchannel gas cooling,” *Proceedings of the Institution of Mechanical Engineers, Part C: Journal of Mechanical Engineering Science*, **236**(9), 5033-5047 (2022). <https://doi.org/10.1177/09544062211057039>
- [24] A.V. Kuznetsov, and A.A. Avramenko, “Effect of small particles on this stability of bioconvection in a suspension of gyrotactic microorganisms in a layer of finite depth,” *International Communications in Heat and Mass Transfer*, **31**(1), 1-10 (2004). [https://doi.org/10.1016/S0735-1933\(03\)00196-9](https://doi.org/10.1016/S0735-1933(03)00196-9)
- [25] U. Khan, N. Ahmed, and S.T. Mohyud-Din, “Influence of viscous dissipation and Joule heating on MHD bio-convection flow over a porous wedge in the presence of nanoparticles and gyrotactic microorganisms,” *Springerplus*, **5**, 1-18 (2016). <https://doi.org/10.1186/s40064-016-3718-8>
- [26] M.J. Uddin, M.N. Kabir, and O.A. Bég, “Computational investigation of Stefan blowing and multiple-slip effects on buoyancy-driven bioconvection nanofluid flow with microorganisms,” *International Journal of Heat and Mass Transfer*, **95**, 116-130 (2016). <https://doi.org/10.1016/j.ijheatmasstransfer.2015.11.015>
- [27] R. Naz, M. Noor, T. Hayat, M. Javed, and A. Alsaedi, “Dynamism of magnetohydrodynamic cross nanofluid with particulars of entropy generation and gyrotactic motile microorganisms,” *International Communications in Heat and Mass Transfer*, **110**, 104431 (2020). <https://doi.org/10.1016/j.icheatmasstransfer.2019.104431>
- [28] F. Aman, W.N.H.W.M. Khazim, and S. Mansur, “Mixed convection flow of a nanofluid containing gyrotactic microorganisms over a stretching/shrinking sheet in the presence of magnetic field,” *J. Phys.: Conf. Ser.* **890**, 012027 (2017). <https://doi.org/10.1088/1742-6596/890/1/012027>

- [29] M. Jawad, F. Mebarek-Oudina, H. Vaidya, and P. Prashar, "Influence of Bioconvection and Thermal Radiation on MHD Williamson Nano Casson Fluid Flow with the Swimming of Gyrotactic Microorganisms Due to Porous Stretching Sheet," *Journal of Nanofluids*, **11**(4), 500-509 (2022). <https://doi.org/10.1166/jon.2022.1863>
- [30] X. Zhang, D. Yang, M.I.U. Rehman, A. Mousa, and A. Hamid, "Numerical simulation of bioconvection radiative flow of Williamson nanofluid past a vertical stretching cylinder with activation energy and swimming microorganisms," *Case Studies in Thermal Engineering*, **33**, 101977 (2022). <https://doi.org/10.1016/j.csite.2022.101977>
- [31] M. Jawad, M.K. Hameed, A. Majeed, and K.S. Nisar, "Arrhenius energy and heat transport activates effect on gyrotactic microorganism flowing in maxwell bio-nanofluid with nield boundary conditions," *Case Studies in Thermal Engineering*, **41**, 102574 (2023). <https://doi.org/10.1016/j.csite.2022.102574>
- [32] M. Jawad, M.K. Hameed, K.S. Nisar, and A.H. Majeed, "Darcy-Forchheimer flow of maxwell nanofluid flow over a porous stretching sheet with Arrhenius activation energy and nield boundary conditions," *Case Studies in Thermal Engineering*, **44**, 102830 (2023). <https://doi.org/10.1016/j.csite.2023.102830>
- [33] M. Jawad, "Insinuation of Arrhenius Energy and Solar Radiation on Electrical Conducting Williamson Nano Fluids Flow with Swimming Microorganism: Completion of Buongiorno's Model," *East European Journal of Physics*, (1), 135-145 (2023). <https://periodicals.karazin.ua/ejpb/article/view/20900/19827>
- [34] M. Jawad, "A Computational Study on Magnetohydrodynamics Stagnation Point Flow of Micropolar Fluids with Buoyancy and Thermal Radiation due to a Vertical Stretching Surface," *Journal of Nanofluids*, **12**, 759-766 (2023). <https://doi.org/10.1166/jon.2023.1958>
- [35] A. Majeed, A. Zeeshan, M. Jawad, and M.S. Alhodaly, "Influence of melting heat transfer and chemical reaction on the flow of non-Newtonian nanofluid with Brownian motion: Advancement in mechanical engineering," *Proceedings of the Institution of Mechanical Engineers, Part E: Journal of Process Mechanical Engineering*, 09544089221145527 (2022). <https://doi.org/10.1177/09544089221145527>

ВПЛИВ БІОКОНВЕКЦІЇ НА ПОТІК НЕНЬЮТОНІВСЬКОЇ ХІМІЧНО РЕАГУЮЧОЇ НАНОРІДИНИ ВІЛЬЯМСОНА ЧЕРЕЗ РОЗТЯГНУТУ ПОВЕРХНЮ З ТЕПЛО-ТА МАСОПЕРЕНОСОМ

Мухаммад Джавад^a, М. Муї-Ур-Рехман^b, Коттаккаран Суппі Нісар^{c,d}

^aКафедра математики, Фейсалабадський університет, Фейсалабад 38000, Пакистан

^bКафедра математики та статистики Університет сільського господарства Фейсалабад, Фейсалабад 38000 Пакистан
^cКафедра математики, Коледж природничих і гуманітарних наук, Алхардж, Університет принца Саттама бін Абдулазіза, Алхардж 11942, Саудівська Аравія

Метою цієї статті є детальне дослідження змішаного конвективного потоку нанорідина Вільямсона за наявності розтягнутої поверхні з різними фізичними ефектами. Вплив броунівського руху та термофорезу є частиною цього дослідження. Крім того, для мотивації проблеми в рівнянні енергії враховуються особливості теплового випромінювання. Для стабільності моделі використовується теорія мікроорганізму. Проведено математичне моделювання. Відповідні функції подібності використовуються для перетворення пари керуючих PDE в набір ODE. Wolfram MATHEMATICA займається чисельним вирішенням трансформованих рівнянь за допомогою схеми зйомки. Вплив параметрів потоку, таких як магнетизм, термофорез, пористість, число Пекле та Льюїса, на швидкість, температуру, об'ємну концентрацію та щільність розподілу мікроорганізмів представлено в таблицях і графіках.

Ключові слова: гіротаксичний мікроорганізм; нанорідина Вільямсона; МГД; біоконвекція; метод стрільби